Research Square

Preprints are preliminary reports that have not undergone peer review.
They should not be considered conclusive, used to inform clinical practice,
or referenced by the media as validated information.

Photocatalytic Degradation of Ammonia with Titania Nanoparticles under UV Light Irradiation

Seyedehfatemeh Hashemi
Semnan University
Samad Sabbaghi (sabbaghi@shirazu.ac.ir)
Shiraz University https://orcid.org/0000-0003-4689-4081
Rahmatallah Saboori
Shiraz University
Bahman Zarenezhad
Semnan University

Research Article

Keywords: Ammonia, Degradation, Efficiency, NPs, Photocatalyst, Titania.

Posted Date: September 2nd, 2021

DOI: https://doi.org/10.21203/rs.3.rs-657725/v1

License: This work is licensed under a Creative Commons Attribution 4.0 International License.
Read Full License

Photocatalytic Degradation of Ammonia with Titania Nanoparticles under UV Light Irradiation

Seyedehfatemeh Hashemi[a], Samad Sabbaghi[b,c,*], Rahmatallah Saboori[c], Bahman Zarenezhad[a]

[a]Department of Chemical Eng., Faculty of Chemical, Petroleum and Gas Engineering, Semnan University, Semnan, Iran.
[b]Nanochemical Engineering Department, Faculty of Advanced Technologies, Shiraz university, Shiraz, Iran.
[c]Drilling Nano Fluid Lab., Shiraz University, Shiraz, Iran

Abstract

Ammonia is one of the most significant contaminants of water resources which make perilous and dire environmental detriment for human life. In this investigation, the photocatalytic degradation of ammonia from an aqueous solution was evaluated with the help of titania nanoparticles. Titania nanoparticles (NPs) were synthesized by sol-gel procedure and also the surface morphology and chemical structure of them was carried out by XRD(X-ray powder diffraction), FTIR(Fourier transform infrared), DLS(Dynamic light scattering), EDX(Energy-dispersive X-ray spectroscopy), FE-SEM(field emission scanning electron microscope), and TEM(Transmission electron microscope) analyses. To elaborate the effect of some parameters including pH, initial concentration of pollutant, catalyst dosage and contact time, Design Expert Software (I optimal technique) was employed. Results demonstrated that titania NPs have a high photocatalytic activity for ammonia removal. Moreover, the pH parameter had the greatest effect on the degradation performance. The optimum amounts of NPs concentration, initial concentration of contaminant, contact time and pH obtained 0.3 g/l, 1500 mg/l, 120 min and 12. NPs were used four times and results showed that the removal efficiency of the NPs decrease from 96.96 % to 65%.

Keywords: Ammonia, Degradation, Efficiency, NPs, Photocatalyst, Titania.

*Corresponding Author: E-mail: sabbaghi@shirazu.ac.ir; samad.sabbaghi@uwaterloo.ca, Tel.: +987136139669, Fax: +987136139662.

1. Introduction

Although ammonia is one of the compounds which is employed in the production of some chemical materials like urea, fertilizer, fiber, plastic, explosives, paper and rubber, it is a common contaminant of water resources which is consist of nitrogen and nutrients that can accelerate the eutrophication and growth of algae in aquatic environments and eventually make some ecological issues (Reli et al. 2015; Shavisi et al. 2014; Shibuya et al. 2013; Zendehzaban et al. 2013). Damage caused by the presence of ammonia in water sources is too vital and dangerous. Ammonia at high concentrations reduces the oxygen of the water and reduces the disinfection efficiency of chlorine and endangers aquatic life and also creates respiratory and skin problems for humans (Lee et al. 2002; Shavisi et al. 2014; Shavisi et al. 2016). As debated by World Health Organization (WHO), drinking water contains 1.5 mg/l of ammonia. So, this level is more than the level that can changes the taste and smell of water.

In the recent decade, water pollution is becoming a global issue in world environmental community researches (Shavisi et al. 2016). Therefore, wastewater treatment like degradation of ammonia from the wastewater is an important subject from an environmental point of view (Shibuya et al. 2013). In order to decrease the concentration of ammonia in wastewater, different types of treatment technique including physical and chemical methods such as biological treatment, ion exchange, breakpoint chlorination, electrochemical process, chemical deposition, adsorption, membrane, and advanced oxidation processes are employed (Zendehzaban et al. 2013). The most impressive technique is biological nitrification/denitrification rather than the other techniques, but has some drawbacks such as needing large types of equipment and having high operating costs. So, it makes secondary contamination and requires secondary purification for their degradation process completion (Lee et al. 2002; Reli et al. 2015). Chemical precipitation and adsorption techniques are

frequently used to degrade low ammonia concentrations, but the drawbacks of chemical precipitation and adsorption method methods might be secondary contamination and being limited by cation ions, respectively (Luo et al. 2015). The ion exchange procedure can eliminate ammonium ions from the wastewater, but the secondary purification problem of the ammonia is not gone away. In the breakpoint of the chlorination technique, by-products of converting aqueous ammonia to nitrogen and residual chlorine have to be treated again (Altomare et al. 2012).

According to the aforementioned disadvantages and drawbacks of techniques, the photocatalytic degradation method has been introduced as an alternative procedure of pollutant removal due to low energy consumption, low operating cost, simple operation, minimum secondary waste generation, and high efficiency (Shavisi et al. 2016; Zendehzaban et al. 2013). Semiconductor compounds like titania NPs, zinc oxide NPs are employed to eliminate pollutants with the help of the photocatalytic technique. TiO_2 NPs have been widely employed as catalysts in the decontamination of aqueous solutions due to good stability, environmental compatibility, photochemical stability, low cost, non-toxicity, high efficiency and oxidation ability of toxic substances (Altomare et al. 2012; Luo et al. 2015; Shavisi et al. 2014).

In semiconductor NPs, the electrons are stimulated by light irradiation and holes are created in the valence band, due to the existence of shifted electrons. The photocatalytic oxidation of titania NPs with light irradiation is as follows (Equation 1) (Zhang et al. 2009):

$$TiO_2 + hv \rightarrow TiO_2 + h^+ + e^- \quad (1)$$

In photocatalytic reactions, there are both reduction and oxidation reactions. The oxidation reaction of H_2O and reduction reaction of O_2 is brought in equations (2) and (3,4), respectively. The production of both reactions is OH radicals which can react with ammonia and generate less hazardous products (Shavisi et al. 2014). According to the previous studies, products of ammonia oxidation can be N_2 (equation 6, 8), NO_2^- or NO_3^- (equation 8).

Moreover, Nitrite (NO_2^-) and Nitrate (NO_3^-) can be reduced and produce N_2 which is a safe product (Liu et al. 2017; Luo et al. 2015). (equations 10 & 11)

Photocatalytic Oxidation:

$$H_2O + h^+ \rightarrow H^+ + OH^- \rightarrow OH^- + h^+ \rightarrow HO^\bullet \quad (2)$$

Photocatalytic Reduction:

$$O_2 + e^- \rightarrow {O_2}^{\bullet -} \quad (3)$$

$${O_2}^{\bullet -} + H_2O \rightarrow H_2O_2 \rightarrow OH^\bullet \quad (4)$$

Ammonia reactions:

$$NH_4OH + H_2O \rightarrow {NH_4}^+ + OH^- + H_2O \rightarrow NH_3 + 2H_2O \quad (5)$$

$${NH_4}^+ + OH^- \rightarrow NH_3 + H_2O \quad (6)$$

$$NH_3 \xrightarrow{OH^\bullet} NH_2 + H_2O \xrightarrow{OH^\bullet} NH + H_2O \xrightarrow{OH^\bullet} N_2 + H_2O \quad (7)$$

$$NH_3 \xrightarrow{OH^\bullet} HONH_2 \xrightarrow{OH^\bullet} NO_2 \xrightarrow{OH^\bullet} {NO_2}^- \xrightarrow{OH^\bullet} {NO_3}^- \quad (8)$$

Oxidize Ammonia:

$$2NH_3 + 6h^+ \rightarrow N_2 + 6H^+ \quad (9)$$

Reduce Nitrate:

$$2{NO_3}^- + 12H^+ + 10e^- \rightarrow N_2 + 6H_2O \quad (10)$$

Reduce Nitrite:

$$2{NO_2}^- + 8H^+ + 6e^- \rightarrow N_2 + 4H_2O \quad (11)$$

The photocatalytic process is displayed in Fig. 1.

Owing to the decomposition of water, radicals are produced that oxidize ammonia pollutants. (Equations 12&13) (Zendehzaban et al. 2013):

$$H_2O + h^+ \rightarrow H^+ + OH^- \quad (12)$$

$$OH^- + h^+ \rightarrow HO^\bullet \quad (13)$$

Fig. 1

TiO_2 was employed as photocatalyst in some research carried out by Toyoda, Li, Mohammadi**,** and Malligavathy to eliminate dye. Toyoda et. al studied the removal of methyleneblue (Toyoda et al. 2004). Li et. al investigated the degradation of methyl orange (MO), rhodamine B (Rho B) and methylene blue (MB) (Li et al. 2019). Mohammadi et.al

eliminated Methylene Blue (Mohammadi et al. 2017) and in the other work, Malligavathy et.al evaluated the removal of congo red dye (Malligavathy et al. 2016).

Recently, several scholars employed various metal oxides as a photocatalyst in photocatalytic degradation. The photocatalytic degradation of ammonia is studied by some researchers. Zendehzaban et. al evaluated the photocatalytic removal of ammonia with the help of TiO_2/Leca (Zendehzaban et al. 2013). In another work, He et. al studied the photocatalytic removal of ammonia by Cu/ZnO/rGO nanocomposite (He et al. 2018). Li et.al removed ammonia by zinc ferrite/activated carbon (Zn Fe_2O_4/AC) (Li et al. 2019). Sharifnia et. al employed TiO_2/perlit (Shavisi et al. 2014), and ZnO/Leca for the degradation of ammonia (Sun et al. 2013). Mohammadi et. al investigated the removal of ammonia by a photocatalyst TiO_2/ZnO immobilized on the Leca base (TiO_2/Leca ZnO) (Mohammadi et al. 2016). Wang et. al used an SL g-C_3N_4 photocatalyst to eliminated ammonia (Wang et al. 2014). Luo et al removed ammonia by using La/Fe/TiO_2 (Luo et al. 2015). Sun et. al studied ammonia removal by Pd/N/ TiO_2 (Sun et al. 2013). Liu et. al evaluated the removal of ammonia using Zn Fe_2O_4/rGO (Liu et al. 2017). Ye et. al employed zinc ferrite/activated carbon (Zn Fe_2O_4/AC) for photocatalytic removal of ammonia (Ye et al. 2019).

There are some studies that are focused on photocatalytic ammonia removal. In this study, there are several differences compare with the other studies. The Design-Expert software is used for finding the various parameters effect on optimum removal of ammonia and reducing the number of experiments while other studies are not used it. This study is carried out in a very high range of concentrations of ammonia (250-1500 mg/l) and in the highest concentration (1500 mg/l), ammonia removal is dramatically significant compared with other studies. The optimum amount of catalyst dose is 0.3 g/l which is very slight. The reuse ability of Nps has been investigated. After four times use, the removal rate was 65% which is indicated that the catalyst is economical to use. Also, in my work the Design Expert software

has been used for finding the effect of single and double parameters on optimum removal of ammonia and reducing the number of experiments while other studies are not used it.

The photocatalytic removal of ammonia investigated by some researchers. As an example, Sharifnia et. al using TiO_2/perlit for removal of ammonia (Shavisi et al. 2014). This work is compared with my work. In this work (Sharifnia et. al) initial concenteration of ammonia is 170 mg/l while in my work, the initial concentration of ammonia is very higher (1500 mg/l), the amount of catalyst is 11.7 g while the amount of my catalyst is 0.3 g/l, and ammonia removal is 68 % after 3 h UV irradiation time while in my work, a dramatical removal equal to 96.96 % is achived. The results of these studies are presented in the results and discussion section (Table 6).

In this study, the effect of titania NPs were examined to evaluate the efficiency of ammonia photocatalytic degradation from an aqueous solution. The titania NPs were synthesized by the sol-gel technique and nanoparticles and were characterized by XRD, FTIR, DLS, EDX, FE-SEM, and TEM analyses. The effect of various parameters such as pH, ammonia concentration, catalyst dosage, contact time, the intensity of UV & visible light irradiation and aeration were investigated on the ammonia elimination and the parameters were optimized.

2. Materials and method

2.1. Materials

Following products including Tetraisopropoxide ($Ti(OCH(CH_3)_2)_4$, TTIP), nitric acid (HNO_3, 65%), ethanol (C_2H_5OH, 99.9%), ammonium hydroxide (NH_4OH, 25%), and hydrochloric acid (HCl, 37%) were provided from Merck company.Moreover, Sodium hydroxide (NaOH) was purchased from the Sinochem company. Deionized water (DW) was manufactured by the Zolal company. Ammonia reagent was prepared by the Hach company (USA) (contains Nessler's Reagent, mineral stabilizer and polyvinyl alcohol).

2.2. Synthesis of titania NPs

The Sol-gel method was used for synthesizing the titania NPs: A mixture of TTIP (5 ml) and ethanol (20 ml) was produced by vigorous magnetic stirrer after 20 min at ambient temperature. After that, the solution was mixed with dilut nitric acid for 5-10 min at ambient temperature, and allowed to form sol and gel. The gel was dried at ambient temperature. At the final step, the powder was calcinated in a reactor at 400 ºC for 4 h (Morgani et al. 2017).

2.3. Investigation of adsorption activity of TiO_2 NPs

The adsorption activity of the nano-TiO_2 in the removal of ammonia from aqueous solution was investigated at the different ammonia concentrations, adsorbent concentration (nano-TiO_2 as an adsorbent), contact time, and pH. To determine the removal efficiency of ammonia, a specific amount of adsorbent was added to ammonia solution at a known pH and then was mixed at the known contact time at ambient conditions. After 120 min, 10 ml of sample was centrifuged. Eventually, ammonia concentration was determined with UV–vis Spectrophotometer Jusco V-730 by adding Nessler's reagent to the sample. The measured absorbance was at the wavelength of 425 nm which is considerable (Niedzielski et al. 2006). The removal percentage of ammonia was calculated by the following equation 14:

$$\text{Ammina removal } (\%) = \frac{C_0 - C_t}{C_0} \times 100 \quad (14)$$

Based on the above equation, the ammonia concentration in solution is shown with C_0 and C_t (mg/L) at t=0 and at a contact time. All experiments were performed in a photocatalytic cylindrical reactor (Fig. 2). The UV lamp (T5-8W) is in the center of the reactor, and the light is reflected in all directions. In the cooling chamber, water is used as a coolant and the temperature was kept at ambient temperature. An aeration pump was employed to create a uniform mixture (Shavisi et al. 2014).

Fig. 2

2.4. Experimental design

The Design-Expert software, version 10, Response Surface Methodology (RSM) (I-optimal) is used to find the effect of various parameters on the optimum condition of ammonia elimination and also to reduce the number of experiments. The effective parameters for degrading ammonia is consist of pH, initial concentration of ammonia, NPs concentration, contact time, and type of light (UV and visible) (Mohammadifard et al. 2019). The number and the values of each level are presented in Table 1.

Table 1

3. Results and Discussion

3.1. Characterization results of NPs

The dried nano-powder was characterized by XRD, FTIR, DLS, EDX, FE-SEM, and TEM analyses. The crystal structure of the sample was characterized by using an X-ray diffractometer and systematic Xpert PRO XRD (λ = 0.178 90 nm) in the range of 400–4000 cm^{-1} with KBr as the reference sample. A PerkinElmer FTIR (model: spectrum RXI)), a TESCAN FE-SEM (model: MIRA III), and a Philips TEM (model: EM 208S), were used to characterize the NPs.

FTIR analysis is employed for organic compounds, but the peak of some other compounds such as metal oxides (TiO_2, ZnO, CuO, etc) can also be seen in FTIR. Fig. 3 shows an FTIR analysis of the prepared TiO_2 NPs. The broad band of 2500 -3600 cm^{-1} (3445 cm^{-1}) and the peak at 1644 cm^{-1} belong to an O–H functional group due to the asymmetrical stretching vibration in H_2O molecules. The band of carbonate groups was in the range of 1400 to 1540 cm^{-1} (1516 cm^{-1}), which is due to the absorption of CO_2 from the atmosphere into the ethanol solution. In the range of 500-1000 cm^{-1}, the Ti-O and Ti-O-Ti bonds have appeared. The FTIR spectrum confirms the stretching vibration peak of Ti-O at 677 cm^{-1} (Morgani et al. 2017; Sidane et al. 2017).

Fig. 3

Fig. 4 demonstrates the XRD pattern of the TiO_2 NPs. The peaks of the anatase TiO_2 NPs are 2θ = 25.5, 37.5, 48, 53, 55 and 62. The planes of (101), (004), (200), (211) and (204) of synthesized TiO_2 catalyst coincide with anatase TiO_2 standard JCPDS Card no. 21-1272 (Zhang et al. 2018). Some weak peaks of the rutile phase are also observed in Fig. 2. presents peaks at 2θ = 27, 36, and 55 correspondings to (110), (101) and (211), planes in rutile TiO_2, respectively (standard JCPDS Card no. 88-1175). According to the XRD patterns, there are mixture peaks of anatase and rutile in the synthesized Titania NPs. The anatase phase is dramatically higher than the rutile phase which is better for photocatalytic reactions (Thamaphat et al. 2008).

Fig. 4

Fig. 5 demonstrates the particle size distribution of TiO_2 nanoparticles by the DLS technique. From Fig. 5, it is observed that the distribution of titanium dioxide particles is narrow with an average particle size of 60 nm (Sadeghalvaad et al. 2015).

Fig. 5

The elemental composition of the TiO_2 NPs was determined using energy-dispersive X-ray spectroscopy (EDX, TESCAN-Vega 3). Fig. 6 shows the EDX analysis of the TiO_2 nanoparticles. The EDX analysis revealed that these particles contain O and Ti elements. The peaks of the Ti and O elements were observed in Fig. 6. The weight percentage of Ti & O atoms is shown in table 2.

Fig. 6

Table 2

The field emission scanning electron microscopy (FE-SEM) and (TEM) micrographs of TiO_2 NPs are shown in Fig. 7 and Fig. 8, respectively.

The size and morphology of TiO_2 NPs were analyzed by FE-SEM measurements. Fig. 7 shows that the prepared TiO_2 has a spherical morphology, and the sizes of NPs are about 55–64 nm. Fig. 7 indicates that the mean size of TiO_2 nanoparticles is about 60 nm.

Fig. 7

The TEM analysis was used for a better view of the TiO_2 NPs. The NPs have a spherical morphology with an average diameter about of 60 nm, which is in good agreement with the XRD and DLS analyses. TEM/EDX analyses confirmed the results obtained by XRD.

Fig. 8

3.2. Statistical analysis and evaluation of experimental results

Design expert software suggested 19 some experiments with the different parameters' values. The experiments were designed and the results for photocatalytic removal of ammonia are shown in Table 3. In statistical analysis of responses, the second-order polynomial equation is used to predict responses based on the considered parameters (Equation 15). The analysis of variance (ANOVA) was used to check the accuracy of the model. F-value (773.34) and P-value (<0.0001) and R^2 (0.99) showed that the model has high accuracy.The amount of P-value for all parameters was tabulated in Table 4 and indicated that all parameters are effective in photocatalytic removal of ammonia (Niedzielski et al. 2006).

$$\text{Ammonia Removal \%} = +37.86 + (22.21 \times A) + (9.38 \times B) + (3.35 \times C) + (12.79 \times D) + (4.31 \times AD) + (6.22 \times B^2) - (6.66 \times C^2) + (6.06 \times D^2) \quad (15)$$

Table 3

Table 4

3.3. Effect of different parameters on the ammonia degradation

The effect of initial ammonia concentration, pH, contact time, photocatalyst dosage and contact time was investigated on the removal of ammonia by using analysis of variance (ANOVA).

The pH of a solution is the most effective parameter (based on F-Value) in the removal of ammonia by the photocatalytic method. The effect of pH on the removal of ammonia from the solution was shown in Fig. 9. It is obvious that, the removal of ammonia enhances from 40 % to about 97 % with increasing pH value from 8 to 12. pH influences the surface charge nanoparticles and also the adsorption of ammonia on the photocatalyst surface and thus the rate of pollutants removal (Zhang et al. 2009).

Fig. 9

According to the following equations (16 & 17), in the presence of H^+ (acidic ambient) and OH^- (alkaline ambient), the surface of TiO_2 can be protonated and deprotonated, respectively. Since the charge of ammonia is positive and the surface of TiO_2 particles at alkali media get a negative charge and cationic types can be easily adsorbed, therefore photodegradation is done better at alkali conditions.

$$TiO_2 + H^+ \rightleftarrows TiOH^{2+} \quad (16)$$

$$TiOH + OH^- \rightleftarrows TiO^- + H_2O \quad (17)$$

$$TiO^- + H^+ \rightarrow TiOH + h^+ \rightarrow TiOH^\bullet \quad (18)$$

$TiOH^\bullet$ is a source of hydroxyl radicals (•OH) to react with ammonia.

$$NH_4OH + H_2O \rightarrow {NH_4}^+ + OH^- + H_2O \quad (19)$$

$$NH_4^+ + OH^- + TiOH^\bullet \rightarrow NH_3 + H_2O + TiOH \quad (20)$$

$$NH_3 \xrightarrow{OH^\bullet} NH_2 + H_2O \xrightarrow{OH^\bullet} NH + H_2O \xrightarrow{OH^\bullet} N_2 + H_2O \quad (21)$$

The point of zero charges (PZC) of TiO_2 NPs is about 6.3 - 6.8 (Shavisi et al. 2014; Gong et al. 2015; Jamil et al. 2016). The point of zero charges is the pH at which the surface of the adsorbent is globally neutral. The Zeta potential of TiO_2 NPs in the range of 4-12 is shown in Table. 5 and Fig. 10. The relationship between zeta potential and the pH values is illustrated in fig. 10. It is obvious that in pH=6.3, the zeta potentials of catalyst is zero (in Smoluchowski model in pH=6.8, zeta potentials of catalyst is zero). Below this value, the

surface is positively charged; beyond this value, it is negatively charged. So normally, it is always easier to adsorb a cation on a negatively charged surface, and an anion on a positively charged surface (Zawawi et al. 2017). Therefore, at pH <pH_{zpc}, the surface charge of the catalyst is positive and at pH> pH_{zpc} it is negative (Shavisi et al. 2014). According to the Table 5, with increasing pH, the surface of the catalyst has become more negative and interaction between the catalyst surface with the available ammonium ions leads to strong absorption and eventually more pollutants are removed (Shavisi et al. 2014). Also, with increasing pH, the number of hydroxyl ions (OH) gradually increased and as a result, more hydroxyl radicals (•OH) are produced which increases the removal efficiency [8]. The ammonia interaction with the photocatalyst surface at pH=12 was optimized and the ammonium ions are adsorbed at the highest surface. Under these conditions, the electron absorption by ammonium ions has resulted in a significant increase in the removal efficiency (Shavisi et al. 2016).

Fig. 10

Table 5

The effect of UV irradiation time on the photocatalytic removal of ammonia contaminant by using TiO_2 as photocatalyst is shown in Fig. 11. Experimental results showed that with increasing the contact time from 20 to 120 min, the removal rate increased from 60 to 96.96%. Residual ammonia decreased with UV irradiation time and it is due to the fact that with the UV irradiation time increment, more hydroxyl radicals (•OH) are produced which causes the performance of removal to enhance (Ghenaatgar et al. 2019). It is noteworthy that in all experiments, the reactor was placed in the dark for 30 min and then exposed to UV light irradiation for 120 min. The observed results are shown that the concentration of remained ammonia in dark conditions, was about 856 mg/l (42.87%). This amount of ammonia which removed from the solution, occurred via the adsorption process (Shavisi et al. 2014). By

313 using titania photocatalyst, 96.96 % of ammonia is removed from the solution after 120 min
314 UV light irradiation (The maximum concentration of ammonia in the final solution was about
315 45 mg/l).

316 **Fig. 11**

317 Another factor that influences ammonia removal is the initial concentration of ammonia. The
318 effect of the initial concentration on the removal is shown in Fig. 12. Results showed that by
319 increasing the initial concentration of ammonia, the removal efficiency increases due to the
320 oxidation of OH^- anions and the generation of •OH radicals. In the concentration of more
321 than 1000 (mg/l), the removal rate rapidly enhances with increasing the initial concentration,
322 because the ammonia pollutant molecules can occupy all active sites of the photocatalyst
323 (Mohsenzadeh et al. 2019).

324 **Fig. 12**

325 An investigation was done on the evaluation of the effect of catalyst dose on the removal of
326 ammonia and results indicated that catalyst dose is a crucial factor in the photocatalytic
327 removal of ammonia. In order to remove the ammonia, the effect of catalyst dose from 0.1 to
328 0.7 g/l was investigated. Fig. 13 shows the effect of catalyst dose on the degradation
329 efficiency. It is obvious that by increasing the catalyst dosage to 0.3 g/l, the number of active
330 sites on the catalyst surface enhances, and this increase causes the interaction between the
331 photocatalyst and the ammonia contaminant, and eventually, the removal rate enhances
332 (Shavisi et al. 2014). Also, the amount of absorbed photon increases and thus increases
333 ammonia removal. At concentrations above 0.3 g/l may be due to inactivation of the active
334 sites, as well as a decrease in the light intensity to the catalyst surface and limited hydroxyl
335 radical ($^{\bullet}OH$) production, the removal rate decreased (Song et al. 2013; Zhang et al. 2009).
336 When the photocatalyst dosage is beyond its optimum amount, the solution becomes turbid
337 and due to agglomeration of the photocatalyst as well as the lack of light penetrating deep

into the solution, the efficiency of removal decreased (Dariani et al. 2016; Koe et al. 2020). Therefore, the optimum value of the catalyst dose is 0.3 g/l.

Fig. 13

3.4. Effect of interaction parameters on the ammonia removal

One of the most advantages of RSM is that it studies the interaction between parameters and their effect on the removal of ammonia. Fig. 14 shows the interaction between contact time and pH (AD) on ammonia removal. This figure shows that the removal rate of ammonia will increase with raising the contact time and pH. According to the analysis of variance (ANOVA) (table 4), there is no interaction between pH and ammonia concentration, so they can be regarded as independent parameters.

Fig. 14

3.5. Optimum condition of ammonia removal

To investigate, the optimum condition for ammonia removal, initial concentration of ammonia, nanoparticle concentration, contact time and pH were considered in the specific ranges (table 1). The initial concentration of ammonia was 1500 mg/l and the removal rate was set to the maximum. The results of ammonia removal in the optimum condition shown in Fig. 15. At the optimum condition, the highest ammonia removal was 96.96% and the highest desirability was 1.000. This optimum condition was repeated three times in the laboratory and the removal efficiency was about 95.94%.

Fig. 15

3.6. Type of light irradiation

Fig. 16 shows the effect of two types of UV and visible light on the photocatalytic removal of ammonia by the TiO_2 photocatalyst. According to the outcomes, the optimum conditions (Fig. 15) under UV and visible light irradiation removal rate was 96.96% and 90.18%,

362 respectively. This indicates that the rate of ammonia removal in the presence of UV light is
363 higher than under the visible light, which is mainly due to the catalytic band gap. The band
364 gap of photocatalyst is 3.2 eV that the UV light performs better than the visible light and the
365 lower the band gap the performance is better in the presence of the Visible light (Anandan et
366 al. 2010). Fig. 17 shows the tauc plot of TiO_2 nanoparticles (Viezbicke et al. 2015). In the
367 photocatalytic process, a metal oxide is activated with UV light, Visible light or sunlight.
368 According to the previous studies, a metal oxide that has a higher Bandgap (Eg) that can
369 absorb over a large region of UV light as compared to Visible light which is because of large
370 excitation binding energy. In many studies, a band gap of rutile and anatase phase is reported
371 about 3.0 eV and 3.2 eV, respectively. The band gap of synthesized photocatalyst is 3.2 eV
372 which is shown that the anatase phase is dramatically higher than the rutile phase. The
373 anatase phase has the highest photocatalytic activity because of an indirect band gap of the
374 anatase phase (Phromma et al. 2020).

375 **Fig. 16**

376 **Fig. 17**

377 **3.7. Effect of aeration on removal**

378 Fig. 18 shows the effect of aeration on the photocatalytic removal of ammonia under
379 optimum conditions (pH=12, catalyst dose=0.3 g/l, contact time=120 min, initial ammonia
380 concentration=1500 mg/l and UV-visible light). The hydroxyl produced from the reduction of
381 O_2 is shown in equationes 3 & 4 (Kolinko et al. 2009). In the aeration condition and also in
382 the absence of air, the removal efficiencies were about 96.96% and 89.86%. It is obvious that
383 oxygen has not a strong effect on the photocatalytic removal of ammonia in an aqueous
384 solution.

385 **Fig. 18**

3.8. Reusability and stability evaluation of TiO_2 nanoparticle

The reusability of the photocatalyst is an important issue and has therefore been considered an essential issue. By using photocatalyst for a long time, its activity decreases, and ammonia molecules may block out some active sites which cover the surface of photocatalyst (Khan et al. 2015).

Investigating the reusability and stability of titania NPs at the initial ammonia concentration of 1500 mg/l, NPs concentration of 0.3 g/L, pH of 12, and contact time of 120 min. Centrifuging the sample solution was carried out at 7000 rpm after 120 min photocatalytic reaction, and the nanoparticles were separated. Then, the separated titania nanoparticles were reused for the next three times. Fig. 19 demonstrates the reusability of TiO_2 NPs for the removal of ammonia at the optimum condition. It is obvious that after four time usage of the NPs, the rate of removal by the photocatalyst reduced and the removal rate decreased from 96.96% to 65% which indicates that the catalyst is economical to use.

Fig. 19

Ammonia removal efficiency is compared with some previous study and removal condition is tabulated in Table 6. Results demonstrated that, ammonia removes under UV or visible light with a higher catalyst amount and irradiation time. However, in the present work, TiO_2 removes 96.96% of ammonia using 0.3 g/l of the catalyst under 2 h UV irradiation. To compare with other studies, the initial concentration of ammonia is very higher, amount of catalyst and irradiation time is lower than the other studies nevertheless removal efficiency is high.

Table 6

4. Conclusion

The photocatalytic process has been regarded as a low-cost process for the purification of pollutants in water and wastewater. Also, the photocatalytic process is one of the most promising processes for efficient, economical, and environmentally friendly water and waste water treatment. The products are often less harmful, and environmentally friendly. In this study, synthesizing the titania nanoparticles was carried out by the sol-gel method, and the NPs were characterized by the XRD, FTIR, DLS, EDX, FE-SEM, and TEM analyses. The photocatalytic performance of synthesized titania NPs on ammonia removal under UV light was studied by Design- Expert software (using the I-Optimal method). Also, the effect of factors such as NPs concentration, contact time, pH, and initial ammonia concentration on the removal of ammonia from solution were investigated and determined the optimum conditions. According to the results, when it comes to removal of ammonia by titania, pH is the most effective parameter. The removal rate increased with increasing pH from 8 to 12 and the highest removal rate was obtained at pH = 12. By increasing the catalyst dosage from 0.1 to 0.3 g/l, the removal rate augmented, and the highest efficiency of removal achieved in the catalyst concentration of 0.3 g/l. The removal rate increased as a result of the contact time enhancement from 30 to 120 min, and initial ammonia concentration from 250 to 1500 mg/l. After 120 min, the removal rate was fixed. A reduction occurred in the removal efficiency of 96.96 % to 65% after four times of reuse.

Ethics approval and consent to participate:

'Not applicable'.

Consent for publication:

'Not applicable'.

Availability of data and materials:

The data that support the plots within this paper and other findings of the current study are available from the corresponding author upon reasonable request.

Conflict of Interest

The authors declare that they have no conflict of interests that influence the work reported in this paper.

Competing financial interests:

The authors declare no competing financial interests.

Funding:

'Not applicable'.

Authors' contributions:

Samad Sabbaghi: Ideation, Conceptualization, Resources, Supervision, Project administration; Funding acquisition, Methodology.

SeyedehFatemeh Hashemi: Conceptualization, Methodology, Software, Formal analysis, Investigation, Writing (original and review), Visualization,

Rahmatallah Saboori: Supervision, Conceptualization, Validation, Visualization, Methodology.

Bahman Zarenezhad: Resources, Supervision, Methodology, Conceptualization,

All authors read and approved the final manuscript.

Acknowledgements:

'Not applicable'.

Declarations of interest:

‘Not applicable’.

References

Altomare M, Chiarello GL, Costa A, Guarino M, Selli E (2012) Photocatalytic abatement of ammonia in nitrogen-containing effluents. Chem Eng J 191: 394-401.

Anandan S, Ohashi N, Miyauchi M (2010) ZnO-based visible-light photocatalyst: Band-gap engineering and multi-electron reduction by co-catalyst. Appl Catal B 100.3-4: 502-509.

Dariani RS, Esmaeili A, Mortezaali A, Dehghanpour S (2016) Photocatalytic reaction and degradation of methylene blue on TiO2 nano-sized particles. Optik 127. 18: 7143-7154.

Ghenaatgar A, Tehrani RM, Khadir A (2019) Photocatalytic degradation and mineralization of dexamethasone using WO3 and ZrO_2 nanoparticles: Optimization of operational parameters and kinetic studies. J Water Process Eng 32 : 100969.

Gong X, Wang H, Yang C, Li Q, Chen X, Hu J (2015) Photocatalytic degradation of high ammonia concentration wastewater by TiO_2. Future Cities Environ 1.1: 1-12.

He S, Hou P, Petropoulos E, Feng Y, Yu Y, Xue L, Yang L (2018) High efficient visible-light photocatalytic performance of Cu/ZnO/rGO nanocomposite for decomposing of aqueous ammonia and treatment of domestic wastewater. Frontiers in chem 6: 219.

Jamil TS, Sharaf El-Deen SEA (2016) Removal of persistent tartrazine dye by photodegradation on TiO_2 nanoparticles enhanced by immobilized calcinated sewage sludge under visible light. Sep Sci Technol 51.10: 1744-1756.

Khan MM, Adil SF, Al-Mayouf A (2015) Metal oxides as photocatalysts. J Saudi Chem Society 462-464.

Koe WS, Lee JW, Chong WC, Pang YL, Sim LC (2020) An overview of photocatalytic degradation: photocatalysts, mechanisms, and development of photocatalytic membrane. Environ Sci Pollut Res 27.3: 2522-2565.

Kolinko PA, Kozlov DV (2009) Products distribution during the gas phase photocatalytic oxidation of ammonia over the various titania based photocatalysts. Appl Catal B 90.1-2 : 126-131

Lee J, Park H, Choi W (2002) Selective Photocatalytic Oxidation of NH_3 to N_2 on Platinized TiO_2 in Water. Environ Sci Technol 36.24: 5462-5468.

Li Y, Wang W, Wang F, Di L, Yang S, Zhu S, Yu F (2019) Enhanced photocatalytic degradation of organic dyes via defect-rich TiO_2 prepared by dielectric barrier discharge plasma. Nanomaterials 9.5: 720.

Liu SQ, Zhu XL, Zhou Y, Meng ZD, Chen ZG, Liu CB (2017) Smart photocatalytic removal of ammonia through molecular recognition of zinc ferrite/reduced graphene oxide hybrid catalyst under visible-light irradiation. Catal Sci Technol 7: 3210–3219.

Luo X, Chen C, Yang J, Wang J, Yan Q, Shi H, Wang C (2015) Characterization of La/Fe/TiO_2 and its photocatalytic performance in ammonia nitrogen wastewater. Int J Environ Res Public Health 12.11: 14626-14639.

Malligavathy M, Iyyapushpam S, Nishanthi ST, Padiyan DP (2016) Optimising the crystallinity of anatase TiO_2 nanospheres for the degradation of Congo red dye. J Exp Nanosci 11.13: 1074-1086.

Mohammadi A, Aliakbarzadeh Karimi A (2017) Methylene blue removal using surface-modified TiO_2 nanoparticles: a comparative study on adsorption and photocatalytic degradation. Journal of Water Environ Sci Technol 2.2: 118-128.

Mohammadi Z, Sharifnia S, Shavisi Y (2016) Photocatalytic degradation of aqueous ammonia by using TiO_2/ZnO/LECA hybrid photocatalyst. Mater Chem Phys. 184: 110-117.

Mohammadifard Z, Saboori R, Mirbagheri NS, Sabbaghi S (2019) Heterogeneous photo-Fenton degradation of formaldehyde using MIL-100 (Fe) under visible light irradiation. Environ Pollut 251:783-791.

Morgani MS, Saboori R, Sabbaghi S (2017) Hydrogen sulfide removal in water-based drilling fluid by metal oxide nanoparticle and ZnO/TiO_2 nanocomposite. Mater Res Express 4.7: 075501.

Mohsenzadeh M, Mirbagheri SA, Sabbaghi S (2019) Degradation of 1, 2-dichloroethane by photocatalysis using immobilized Pani- TiO_2 nano-photocatalyst. Environ Sci Pollut Res 26.30: 31328-31343.

Niedzielski P, Kurzyca I, Siepak J (2006) A new tool for inorganic nitrogen speciation study: Simultaneous determination of ammonium ion, nitrite and nitrate by ion chromatography with post-column ammonium derivatization by Nessler reagent and diode-array detection in rain water samples. Anal Chim Acta 577.2: 220-224.

Phromma S, Wutikhun T, Kasamechonchung P, Eksangsri T, Sapcharoenkun C (2020) Effect of Calcination Temperature on Photocatalytic Activity of Synthesized TiO_2 Nanoparticles via Wet Ball Milling Sol-Gel Method. Applied Sciences 10.3: 993.

Reli M, Ambrožová N, Šihor M, Matějová L, Čapek L, Obalová L, Kočí K (2015) Novel cerium doped titania catalysts for photocatalytic decomposition of ammonia. Appl Catal B 178: 108-116.
Sadeghalvaad M, Sabbaghi S (2015) The effect of the TiO_2/polyacrylamide nanocomposite on water-based drilling fluid properties. Powder Technol 272: 113-119.
Shavisi Y, Sharifnia S, Hosseini S, Khadivi M (2014) Application of TiO_2/perlite photocatalysis for degradation of ammonia in wastewater. J Ind Eng Chem 20.1: 278-283.
Shavisi Y, Sharifnia S, Mohamadi Z (2016) Solar-light-harvesting degradation of aqueous ammonia by CuO/ZnO immobilized on pottery plate: Linear kinetic modeling for adsorption and photocatalysis process. J Environ Chem Eng 4.3: 2736-2744.
Shavisi Y, Sharifnia S, Zendehzaban M, Mirghavami M L, & Kakehazar S (2014) Application of solar light for degradation of ammonia in petrochemical wastewater by a floating TiO_2/LECA photocatalyst. J Ind Eng Chem 20.5: 2806-2813.
Shibuya S, Aoki S, Sekine Y, Mikami I (2013) Influence of oxygen addition on photocatalytic oxidation of aqueous ammonia over platinum-loaded TiO_2. Appl Catal B 138-139: 294-298.
Sidane D, Khireddine H, Bir F, Yala S, Montagne A, Chicot D (2017) Hydroxyapatite-TiO_2-SiO_2-coated 316L stainless steel for biomedical application. Metall Mater Trans A 48.7: 3570-3582.
Song KS, Yu XC, Hu DD, Zheng X, Guo JY (2013) Photocatalytic Degradation of Ammonia Nitrogen in Aquaculture Wastewater by Using Nano-ZnO, Adv. Mat. Res. 610 (2013) 564-568.
Sun D, Sun W, Yang W, Li Q, Shang JK (2015) Efficient photocatalytic removal of aqueous NH_4^+–NH_3 by palladium-modified nitrogen-doped titanium oxide nanoparticles under visible light illumination, even in weak alkaline solutions. Chem Eng J 264: 728-734.
Thamaphat K, Limsuwan P, Ngotawornchai B (2008) Phase characterization of TiO_2 powder by XRD and TEM. Kasetsart J (Nat. Sci.) 42.5: 357-361.
Toyoda M, Nanbu Y, Nakazawa Y, Hirano M, Inagaki M (2004) Effect of crystallinity of anatase on photoactivity for methyleneblue decomposition in water. Appl Catal B: Environ 49.4: 227-232.
Viezbicke BD, Patel S, Davis BE, Birnie III DP (2015) Evaluation of the Tauc method for optical absorption edge determination: ZnO thin films as a model system. Phys Status Solidi B 252.8: 1700-1710.
Wang H, Su Y, Zhao HX, Yu HT, Chen S, Zhang YB (2014) Photocatalytic oxidation of aqueous ammonia using atomic single layer graphitic-C_3N_4. Environ Sci Technol 48: 11984–11990.
Ye J, Liu SQ, Liu WX, Meng ZD, Luo L, Chen F, Zhou J (2019) Photocatalytic Simultaneous Removal of Nitrite and Ammonia via a Zinc Ferrite/Activated Carbon Hybrid Catalyst under UV–Visible Irradiation. ACS omega 4.4: 6411-6420.
Zawawi A, Ramli RM, Yub Harun N (2017) Photodegradation of 1-butyl-3-methylimidazolium chloride [Bmim] Cl via synergistic effect of adsorption–photodegradation of Fe-TiO_2/AC. Technol 5.4: 82.
Zendehzaban M, Sharifnia S, Hosseini SN (2013) Photocatalytic degradation of ammonia by light expanded clay aggregate (LECA)-coating of TiO_2 nanoparticles. Korean J Chem Eng 30.3: 574-579.
Zhang F, Feng C, Jin Y, Li W, Hao G, Cui J (2009) Photocatalytic degradation of ammonia nitrogen with suspended TiO_2, Bioinform. Biomed Eng 3rd International Conference on pp 1-4.
Zhang H, Wang X, Li N, Xia J, Meng Q, Ding J, Lu J (2018) Synthesis and characterization of TiO_2/graphene oxide nanocomposites for photoreduction of heavy metal ions in reverse osmosis concentrate. RSC Adv 8. 60: 34241-34251.

Table Captions:

Table 1: Levels for each parameter.

Table 2: The elemental composition of the TiO_2

Table 3: Rresponse surface methodology for photocatalytic removal of ammonia.

Table 4: Analysis of variance (ANOVA) photocatalytic removal of ammonia.

Table 5: Zeta potential values of the TiO_2

Table 6: Comparison of ammonia removal efficiency (%) using various photocatalysts.

563
564

Table 1

Name	Units	Levels						
		Levels	**1**	**2**	**3**	**4**	**5**	**6**
Initial ammonia concentration	mg/l	6	250	500	750	1000	1250	1500
Nano particle concentration	g/l	4	0.1	0.3	0.5	0.7	--	--
pH	--	3	8	10	12	--	--	--
Contact time	min	4	30	60	90	120	--	--

565

566

Table 2

Element	Wt %	A %
Ti	46.48	22.49
O	53.52	77.51

567

568

Table 3

Run	A: pH	B: Initial ammonia concentration (mg/l)	C: Nano particle concentration (g/l)	D: Contact time (min)	Removal (%)
1	8	250	0.3	30	8.84
2	8	1500	0.5	120	46.92
3	8	250	0.7	90	14.33
4	10	1000	0.1	30	24.76
5	12	250	0.7	120	76.93
6	12	1500	0.7	90	79.24
7	12	1500	0.3	120	97.25
8	12	1500	0.1	30	54.78
9	8	1500	0.1	60	18.58
10	10	1000	0.7	120	54.18
11	12	250	0.7	30	42.40
12	12	250	0.1	30	34.97
13	10	250	0.3	90	35.35
14	8	1500	0.7	30	24.40
15	12	750	0.3	90	63.38
16	10	250	0.3	90	38.74
17	8	250	0.1	120	16.98
18	8	1000	0.3	90	18.70
19	12	750	0.3	90	63.08

569

570 **Table 4**

	Sum of squares	df	Average of squares	F-Value	P-Value (Probe>F)
Model	11159.66	8	1394.96	773.34	< 0.0001
A: pH	7193.62	1	7193.62	3988.01	< 0.0001
B :Initial ammonia concentration	1166.94	1	1166.94	646.93	< 0.0001
C: Nano particle concentration	100.96	1	100.96	55.97	< 0.0001
D: Contact time	1533.46	1	1533.46	850.12	< 0.0001
AD	148.75	1	148.75	82.47	< 0.0001
B^2	117.50	1	117.50	65.14	< 0.0001
C^2	110.41	1	110.41	61.21	< 0.0001
D^2	112.30	1	112.30	62.26	< 0.0001

571

572

573

574 **Table 5**

pH	Zeta Potential (mv)
4	+ 40
5	+ 22
6.3	0
7	- 10
8	- 32.2
9	- 40.5
0	- 45.3
11	- 49.7
12	- 53.2

575

576

577

578

579

580

581

582

583

584

Table 6

Photocatalyst	Removal conditions	Ref
TiO_2/perlite	Concentration: 170 mg/l Catalyst amount: 11.7 g Irradiation time: 3 h (UV light 125 W) Removal: 68 %	[6]
SL g-C_3N_4	Concentration: 1.5 mg/l Irradiation time: 6 h (UV light) Removal: 80 %	[18]
Pd/N/TiO_2	Irradiation time: 2 h (Visible light) Removal: 80 %	[16]
La/Fe/TiO_2	Concentration: 100.67 mg/l Irradiation time: 5 h (UV light) Removal: 64.6 %	[8]
TiO_2-ZnO/LECA	Concentration: 400 mg/l Catalyst amount: 25 g/l Irradiation time: 3 h (Visible light) Removal: 95.2 %	[17]
Zn Fe_2O_4/rGO	Concentration: 100 mg/l Irradiation time: 4 h (Visible light) Removal: 92.3 %	[19]
Cu/ZnO/rGO	Concentration: 50 mg/l Catalyst amount: 2 g Irradiation time: 2 h (Visible light: Xe lamp) Removal: 83.2 %	[15]
Zn Fe_2O_4/AC	Concentration : 100 mg/l Catalyst amount: 25 g/l Irradiation time: 3 h (UV- Visible light) Removal: 90 %	[20]
TiO_2	Concentration: 1500 mg/l Catalyst amount: 0.3 g/l Irradiation time: 2 h (UV light) Removal: 96.96 %	Present work

585

586

587

588

589

590

Figure Captions:

Fig. 1: The photocatalytic process

Fig. 2: Schematic of the reactor system.

Fig. 3: FTIR pattern of the TiO_2 nanoparticles.

Fig. 4: XRD pattern of the TiO_2 nanoparticles.

Fig. 5: Particle size distribution of TiO_2 nanoparticles.

Fig. 6: EDX analysis of the TiO_2 nanoparticles.

Fig. 7: FE-SEM image of the TiO_2 nanoparticles.

Fig. 8: TEM image of TiO_2

Fig. 9: Effect of pH on ammonia removal at initial ammonia concentration = 1500 mg/l, nanoparticle concentration = 0.3 g/l and contact time = 120 min.

Fig. 10: Zeta potentials versus pH of the TiO_2 nanoparticles.

Fig. 11: Effect of contact time on removal of ammonia at pH = 12, initial ammonia concentration = 1500 mg/l and nanoparticle concentration = 0.3 g/l.

Fig. 12: Effect of initial concentration of ammonia on removal at pH = 12, nanoparticle concentration = 0.3 g/l and contact time = 120 min.

Fig. 13: Effect of catalyst dose on removal of ammonia at pH = 12, initial ammonia concentration = 1500 mg/l and contact time = 120 min.

Fig. 14: Effect of interaction between pH and contact time on ammonia removal.

Fig. 15: Optimum condition for ammonia removal by TiO_2 nanoparticle

Fig. 16: Effect of two types of UV and visible light on removal of ammonia at pH = 12, initial ammonia concentration = 1500 mg/l, nanoparticle concentration = 0.3 g/l and contact time = 120 min.

Fig. 17: Tauc plot for band gap determination of TiO_2 nanoparticle.

Fig. 18: Effect of aeration on removal of ammonia at pH = 12, initial ammonia concentration = 1500 mg/l, nanoparticle concentration = 0.3 g/l and contact time = 120 min.

Fig. 19: Reusability of TiO_2 nanoparticle for ammonia removal after each cycle in optimum condition.

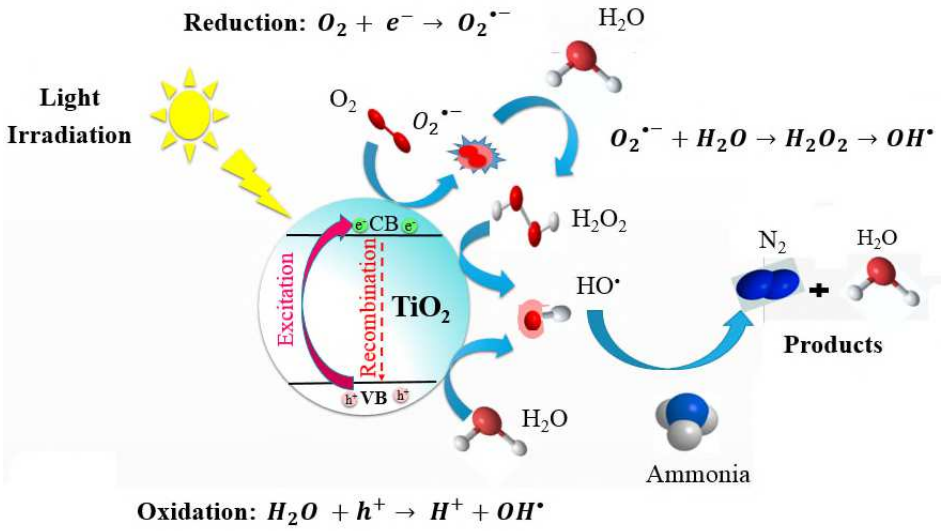
Reduction: $O_2 + e^- \rightarrow O_2^{\bullet -}$
H_2O
Light Irradiation
O_2
$O_2^{\bullet -}$
$O_2^{\bullet -} + H_2O \rightarrow H_2O_2 \rightarrow OH^{\bullet}$
H_2O_2
N_2
H_2O
HO•
Products
e⁻ CB e⁻
Excitation
Recombination
TiO_2
h⁺ VB h⁺
H_2O
Ammonia
Oxidation: $H_2O + h^+ \rightarrow H^+ + OH^{\bullet}$

Fig. 1

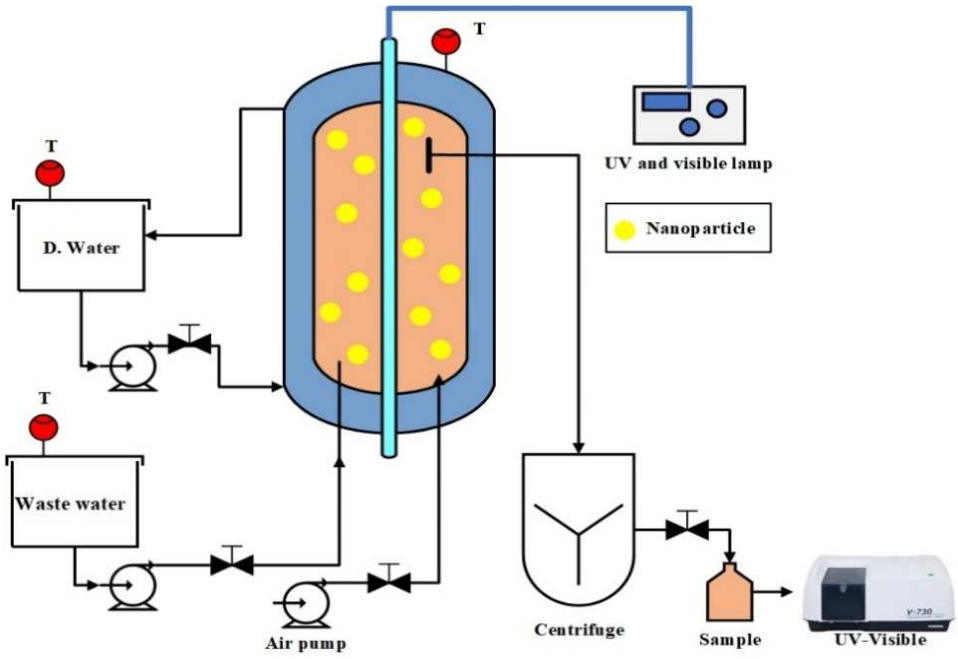
T
UV and visible lamp
Nanoparticle
T
D. Water
T
Waste water
Air pump
Centrifuge
Sample
UV-Visible

Fig. 2

633

634

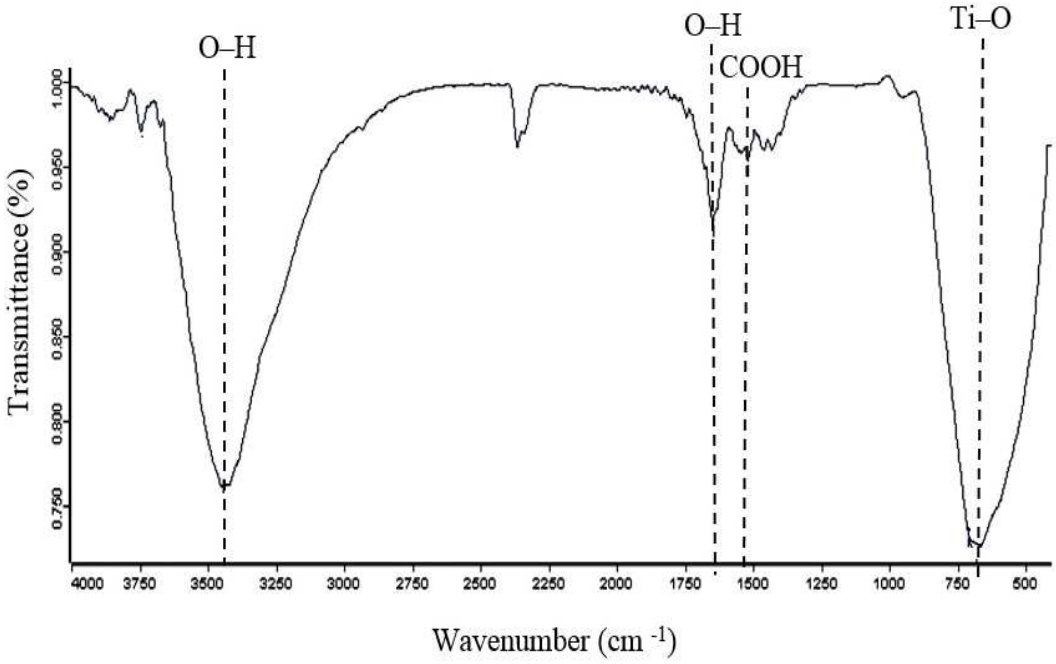

635

636 **Fig. 3**

637

638

639

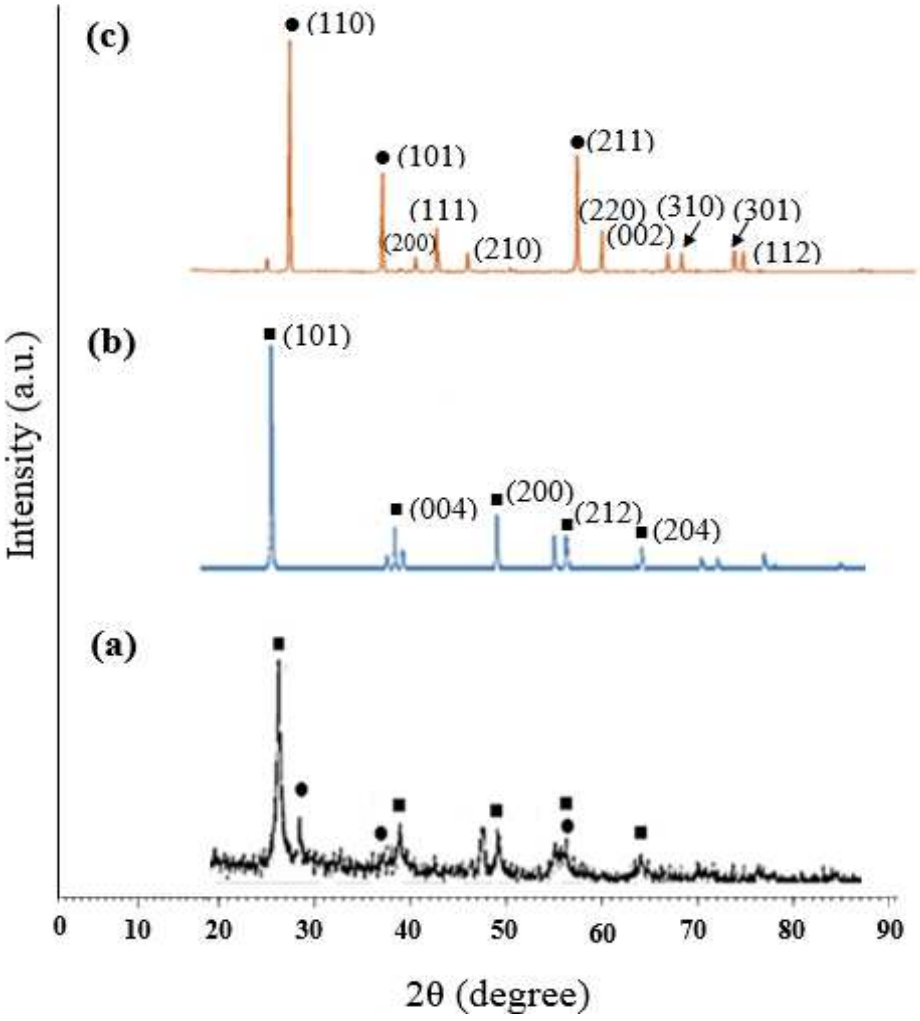
(c)
(110)
(101)
(211)
(111)
(200)
(210)
(220)
(310)
(301)
(002)
(112)
(b)
(101)
(004)
(200)
(212)
(204)
(a)
Intensity (a.u.)
0
10
20
30
40
50
60
70
80
90
2θ (degree)

Fig. 4

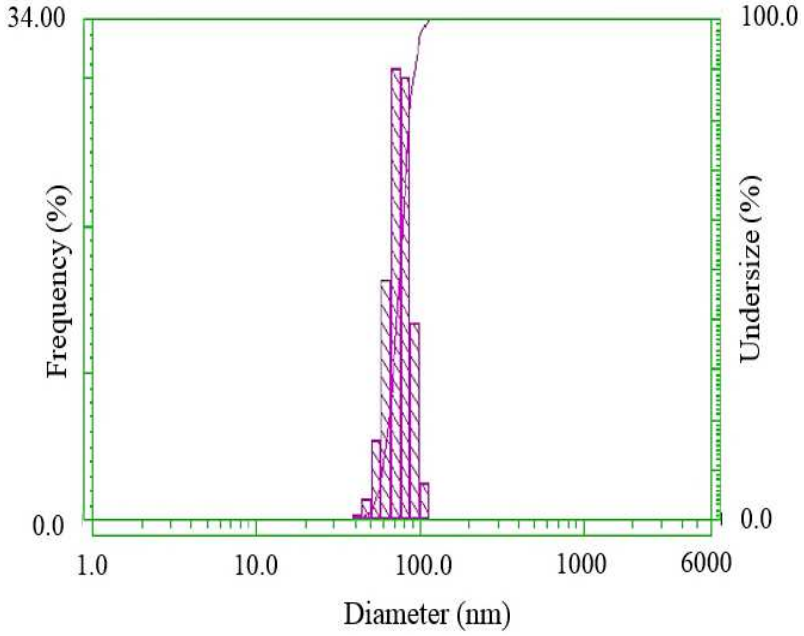

654

655 **Fig. 5**

656

657

658

659

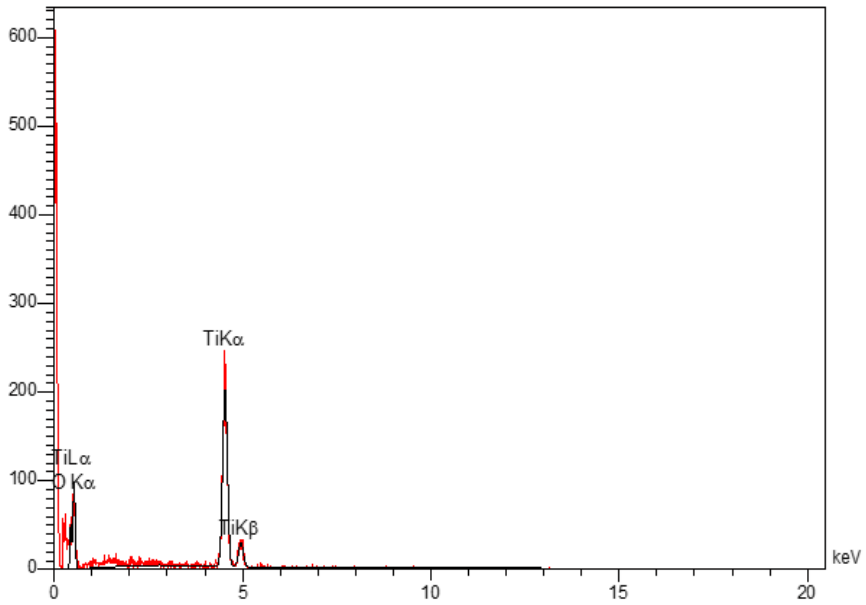

660

661 **Fig. 6**

662

663

664

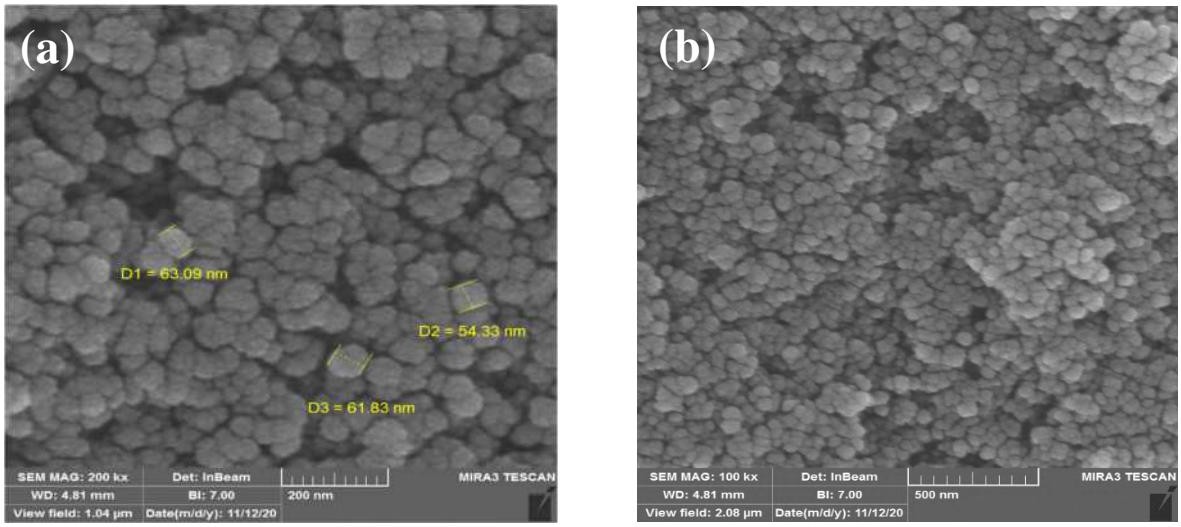
(a)
D1 = 63.09 nm
D2 = 54.33 nm
D3 = 61.83 nm
SEM MAG: 200 kx
Det: InBeam
MIRA3 TESCAN
WD: 4.81 mm
BI: 7.00
200 nm
View field: 1.04 µm
Date(m/d/y): 11/12/20
(b)
SEM MAG: 100 kx
Det: InBeam
MIRA3 TESCAN
WD: 4.81 mm
BI: 7.00
500 nm
View field: 2.08 µm
Date(m/d/y): 11/12/20

Fig. 7

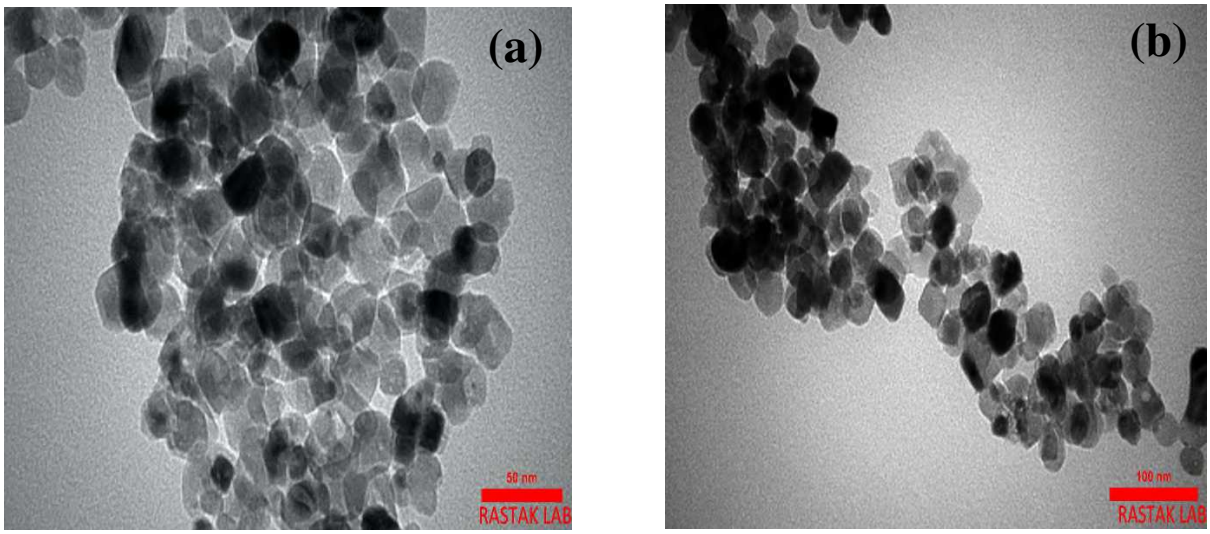
(a)
50 nm
RASTAK LAB
(b)
100 nm
RASTAK LAB

Fig. 8

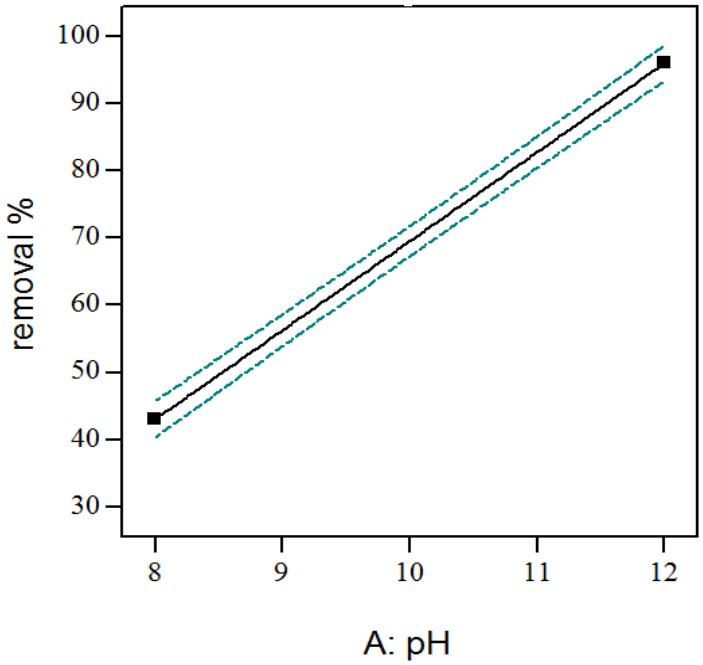
removal %
100
90
80
70
60
50
40
30
8
9
10
11
12
A: pH

Fig. 9

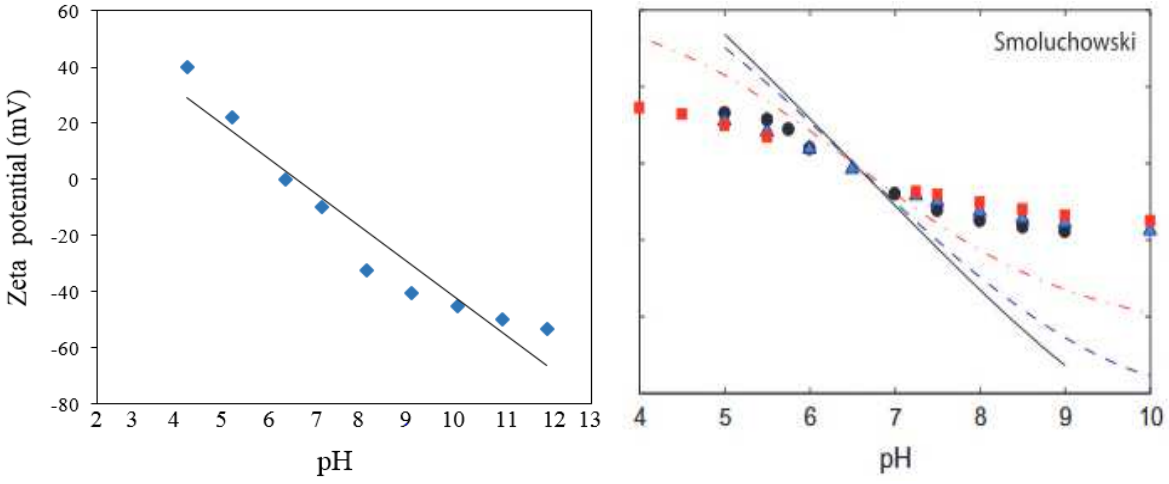
Zeta potential (mV)
60
40
20
0
-20
-40
-60
-80
2 3 4 5 6 7 8 9 10 11 12 13
pH
Smoluchowski
4 5 6 7 8 9 10
pH

Fig. 10

692

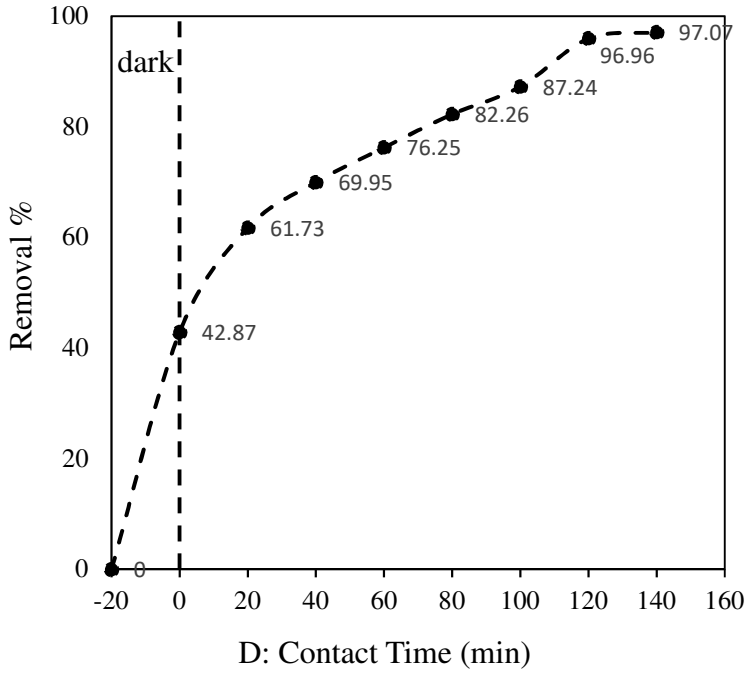

693

694 **Fig. 11**

695

696

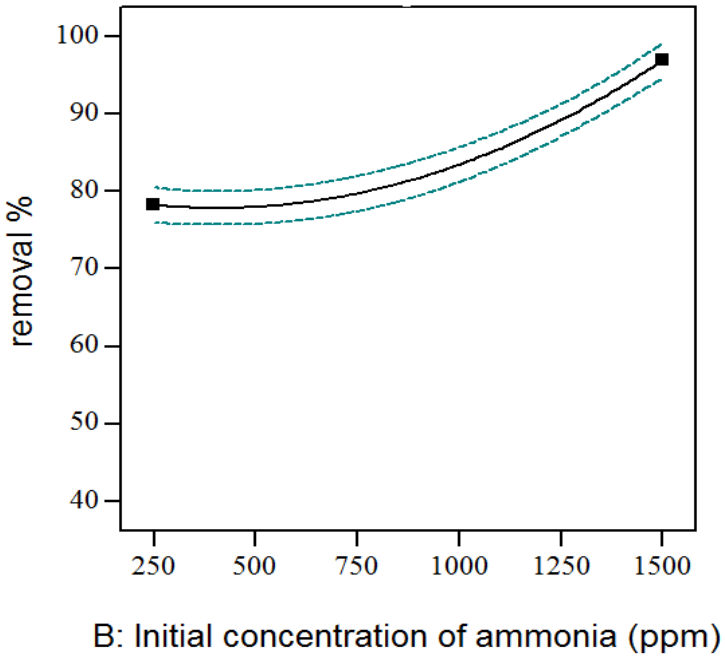

697

698 **Fig. 12**

699

700

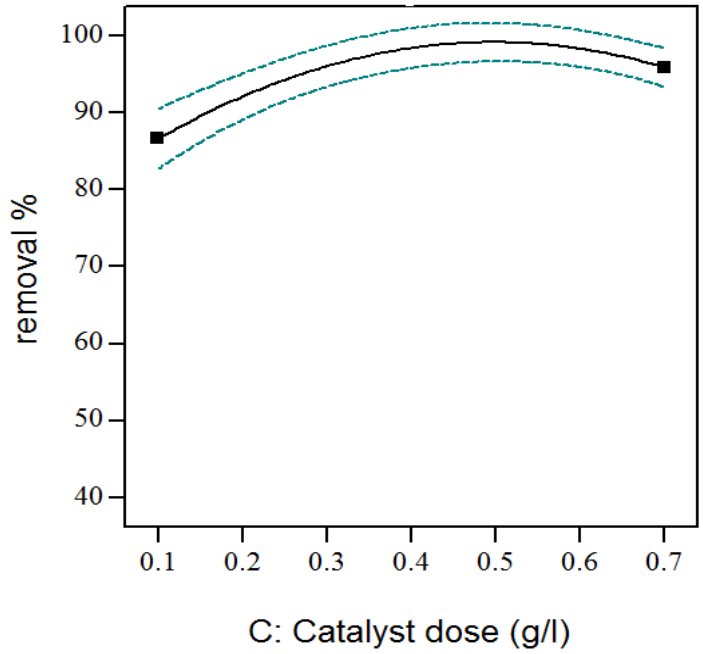
100
90
80
70
60
50
40
removal %
0.1
0.2
0.3
0.4
0.5
0.6
0.7
C: Catalyst dose (g/l)

Fig. 13

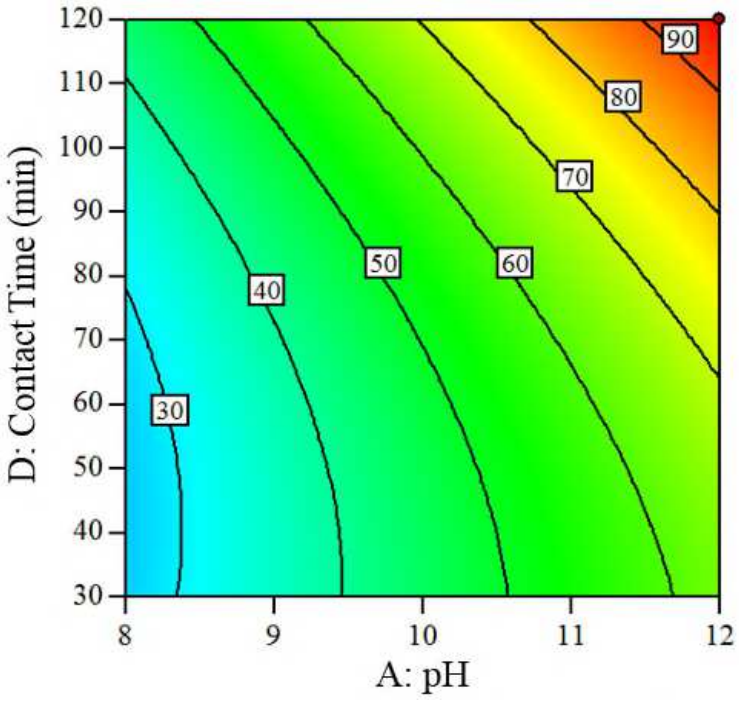
120
110
100
90
80
70
60
50
40
30
D: Contact Time (min)
8
9
10
11
12
A: pH
30
40
50
60
70
80
90

Fig. 14

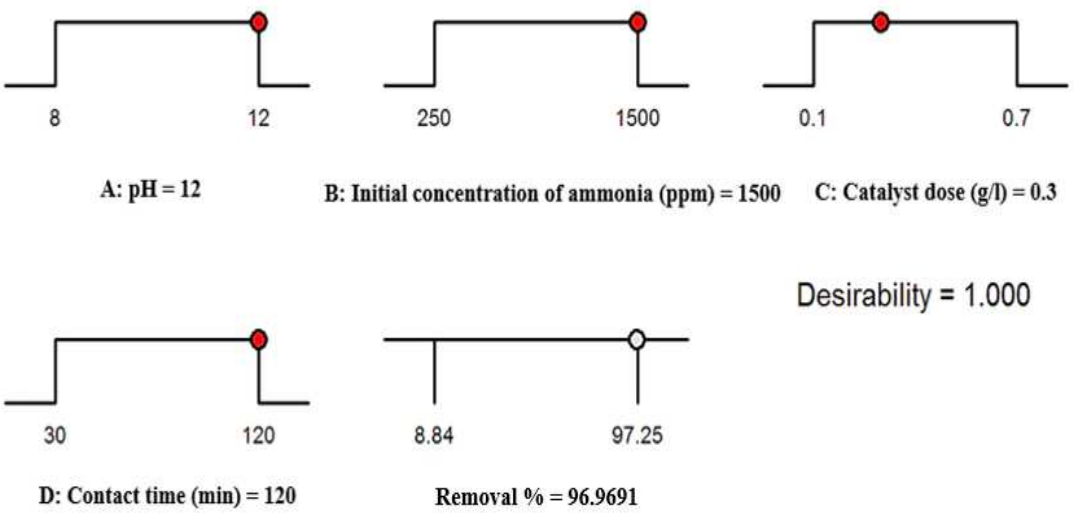

710

711 **Fig. 15**

712

713

714

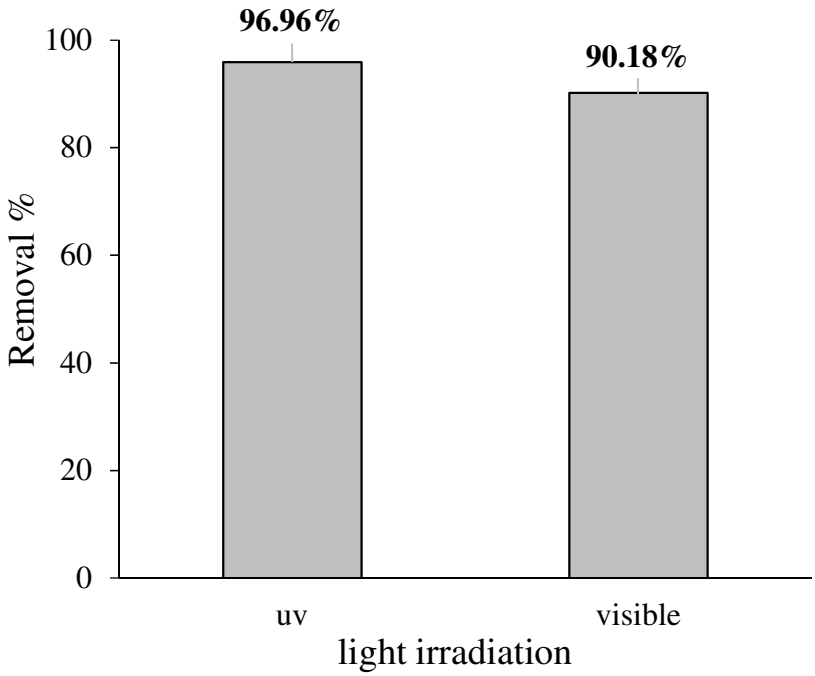

715

716 **Fig. 16**

717

718

719

720

721

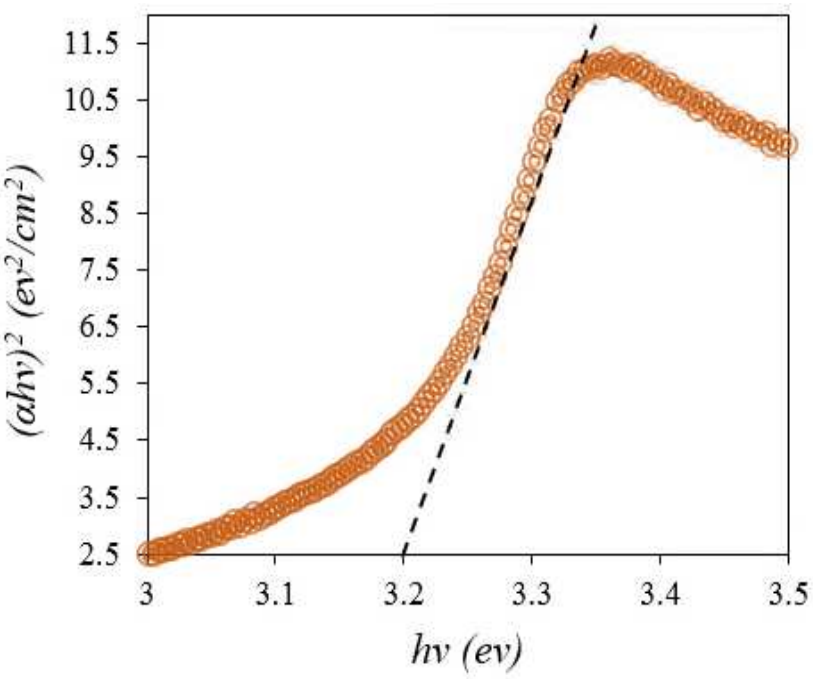
11.5
10.5
9.5
8.5
7.5
6.5
5.5
4.5
3.5
2.5
(αhv)² (ev²/cm²)
3
3.1
3.2
3.3
3.4
3.5
hv (ev)

Fig. 17

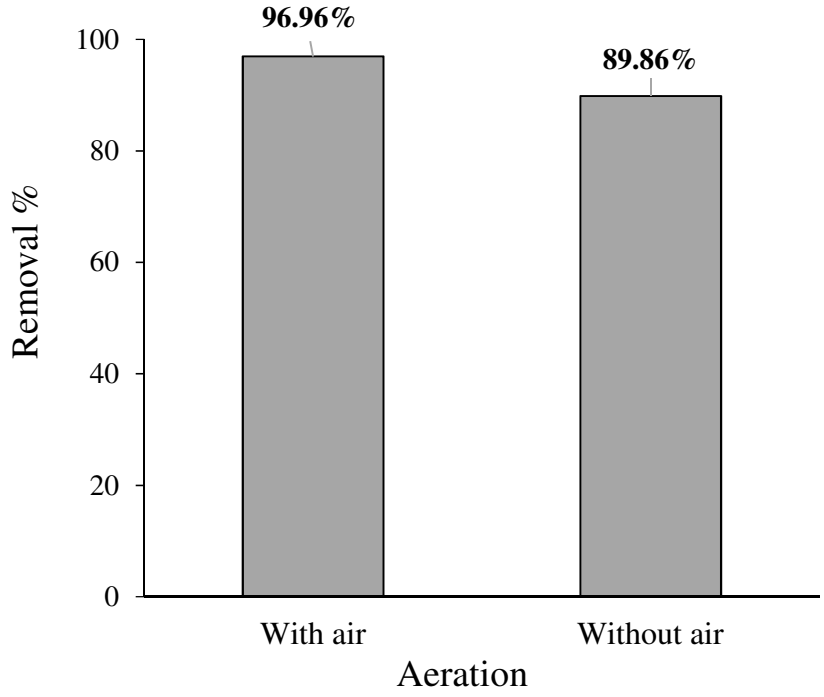
96.96%
89.86%
100
80
60
40
20
0
Removal %
With air
Without air
Aeration

Fig. 18

730

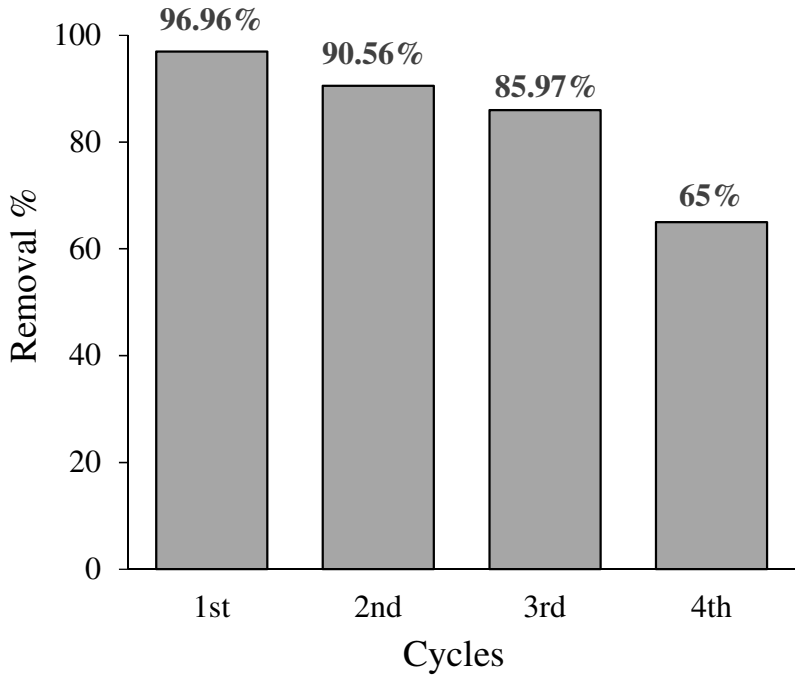

731

732 **Fig. 19**

733

734

735

736

737

738

739

Supplementary Files

This is a list of supplementary files associated with this preprint. Click to download.

- Graphicalabstract.docx